BJR
© 2020 The Authors. Published by the British Institute of Radiology
https://doi.org/10.1259/bjr.20190467

Received: 23 May 2019 | Revised: 17 December 2019 | Accepted: 19 December 2019

Cite this article as:
Lehman VT, Black DF, DeLone DR, Blezek DJ, Kaufmann TJ, Brinjikji W, et al. Current concepts of cross-sectional and functional anatomy of the cerebellum: a pictorial review and atlas. *Br J Radiol* 2020; **93**: 20190467.

## PICTORIAL REVIEW

# Current concepts of cross-sectional and functional anatomy of the cerebellum: a pictorial review and atlas

**VANCE T. LEHMAN, MD, DAVID F. BLACK, MD, DAVID R. DELONE, MD, DANIEL J. BLEZEK, PhD, TIMOTHY J. KAUFMANN, MD, WALEED BRINJIKJI, MD and KIRK M. WELKER, MD**

Department of Radiology, Mayo Clinic, Rochester, Minnesota, United States

Address correspondence to: Dr Vance T. Lehman
E-mail: *Lehman.vance@mayo.edu*

**ABSTRACT**

Recognition of key concepts of structural and functional anatomy of the cerebellum can facilitate image interpretation and clinical correlation. Recently, the human brain mapping literature has increased our understanding of cerebellar anatomy, function, connectivity with the cerebrum, and significance of lesions involving specific areas.

Both the common names and numerically based Schmahmann classifications of cerebellar lobules are illustrated. Anatomic patterns, or signs, of key fissures and white matter branching are introduced to facilitate easy recognition of the major anatomic features. Color-coded overlays of cross-sectional imaging are provided for reference of more complex detail. Examples of exquisite detail of structural and functional cerebellar anatomy at 7 T MRI are also depicted. The functions of the cerebellum are manifold with the majority of areas involved with non-motor association function. Key concepts of lesion–symptom mapping which correlates lesion location to clinical manifestation are introduced, emphasizing that lesions in most areas of the cerebellum are associated with predominantly non-motor deficits. Clinical correlation is reinforced with examples of intrinsic pathologic derangement of cerebellar anatomy and altered functional connectivity due to pathology of the cerebral hemisphere. The purpose of this pictorial review is to illustrate basic concepts of these topics in a cross-sectional imaging-based format that can be easily understood and applied by radiologists.

## INTRODUCTION

The structural and functional anatomy of the cerebellum is complex, but demonstrates reproducible spatial organization. Detail of cerebellar pathologic derangement is often underemphasized in radiology education and reports, but recognition of key concepts and patterns can facilitate image interpretation and clinical correlation. In recent decades, advances in the human brain mapping literature has increased our understanding of anatomy, function, and the clinical significance of lesions involving specific areas of the cerebellum. The purpose of this pictorial review is to illustrate basic concepts of these imaging topics to facilitate application to clinical practice and to the appraisal of human brain mapping research. To do this, key patterns, or signs, of white matter branching and fissure prominence, configuration, and orientation are presented to depict the major anatomic features. Color-coded overlays are provided for reference of further anatomic detail. A brief introduction to relevant embryology and correlation to general vascular territories are provided. Functional organization is presented with blood oxygen level dependent (BOLD) fMRI signal and introduction of lesion–symptom mapping.

## OVERVIEW OF CROSS-SECTIONAL ANATOMY

The cerebellum broadly consists of cortex, central white matter, and deep nuclei. The cortex lacks areas of highly distinct cytoarchitecture analogous to the Brodmann areas of the brain. However, differences in biochemistry and function occur within sagittally oriented segments that have been divided into zones/stripes and modules with a medial to lateral gradient of connectivity to the inferior olives and deep nuclei.[1] The trilaminar cortical layers can be remembered with the pneumonic MPG (superficial to deep: molecular, Purkinje, and granular); the molecular and granular layers have been visualized *in vivo* with specialized techniques at 7 T, but are not routinely visualized in current clinical practice.[2] The Purkinje layer is too small to visualize *in vivo* with current techniques, but serves as the cortical output to the deep nuclei.

The central white matter (corpus medullare) has distinct branching patterns (arbor vitae); of these several particularly prominent white matter stems can be used to

Figure 1. Illustration of the lobes and lobules of the cerebellum with both common names and enumeration per the Schmahmann classification. The color patterns of the lobules and fissures match those in subsequent figures. Note that the precise definitions and nomenclature of individual lobules and even the lobes vary in the literature.

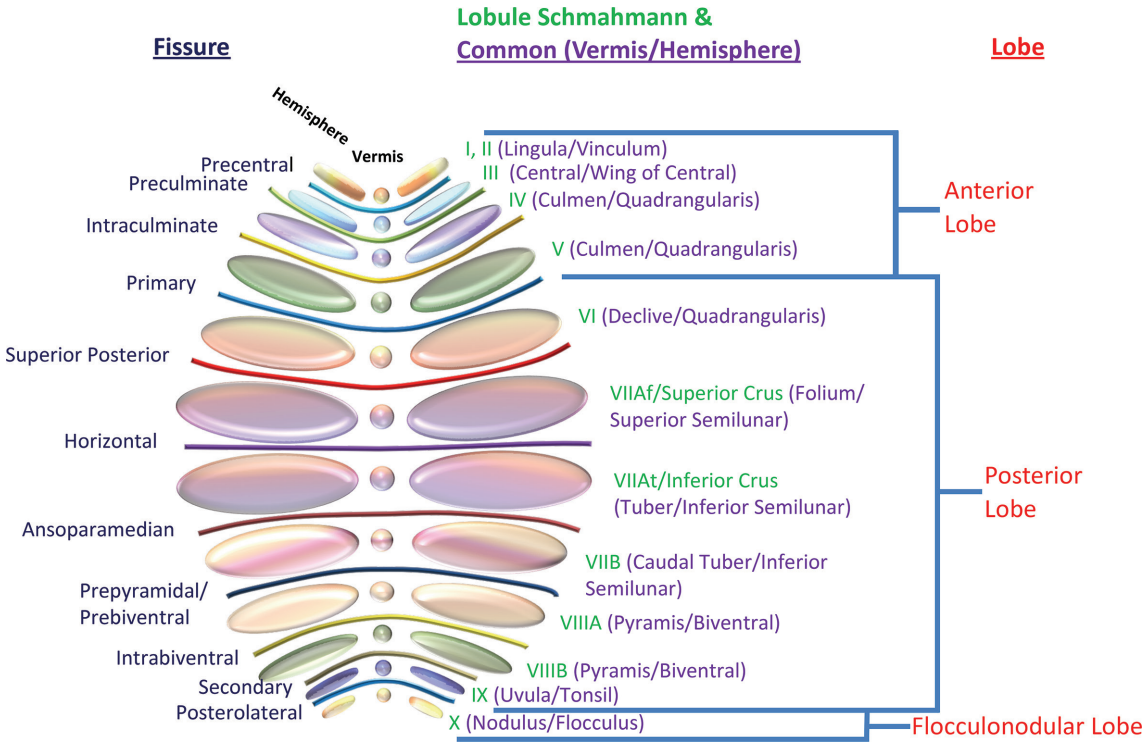


identify key anatomic areas. The deep nuclei give rise to the major efferent white matter fibers. While the dentate nucleus is commonly visualized at 1.5 or 3 T MRI, the interposed and fastigial nuclei are more challenging to visualize even at higher field strength.[3,4]

Side-to-side, the cerebellum is divided into two hemispheres with a midline vermis. Both the hemispheres and the vermis are typically divided into three lobes. In turn, fissures subdivide the lobes into numerous lobules (Figures 1–5). Importantly, the designation of 'anterior' and 'posterior' location for both the lobes and axis of development (below) reflect 'cranial' and 'caudal' location respectively rather than designations by conventional clinical MRI terminology. While the radiologist may be familiar with the common names of the lobes and lobules, numerous nomenclature schemes and definitions exist which can create some confusion. To address this variability, Schmahmann et al proposed a numerical nomenclature which is commonly used in the human brain mapping literature and emerging in the imaging literature.[5,6] Assessment of this level of detail can be important since function and predisposition to certain pathology varies amongst the lobules. Recognition of lobule anatomy also facilitates assessment of congenital anomalies. The Schmahmann classification simplifies lobule nomenclature as the lobules are arranged in numerical order (I–X) radially in the sagittal plane. In many locations, the lobule can be identified quickly on cross-sectional imaging by the relationship to patterns, or signs, of key fissures or white matter stems presented in the figures of this essay. Several methods of automated parcellation of the cerebellar lobules which could aid visual identification and assessment have been described, but these are not yet widely evaluated or implemented in clinical practice.[7]

## EMBRYOLOGY

The development of the cerebellum is highly complex and the details are beyond the scope of this review. Barkovich et al have provided an in-depth analysis with a comprehensive classification system of congenital anomalies.[8] In brief, both the cerebellum and brainstem (pons and medulla) are derived from the rhombencephalon. The fissures appear in sequence, with the primary and posterolateral fissures (separating the lobes) developing first while those separating lobules VI, VIIA, and VIIB (which are the only lobules to share a common white matter stem in the vermis) are the last to form.[6] Understanding this sequence can facilitate interpretation of expected findings on prenatal imaging and avert a misdiagnosis of hypoplasia prior to final differentiation of the lobules.[6] There is both anteroposterior (craniocaudal) and dorsoventral hindbrain patterning; abnormalities of these processes can lead to deranged anatomy along the respective axes.[8] Importantly, lobular development does not occur in the numeric sequence outlined in the Schmahmann classification. Further, the vermis does not arise from fusion of the cerebellar hemispheres, but is derived from dedicated primordium, with the anterior and posterior segments arising separately.[6] These concepts

Figure 2. Three-dimensional surface shaded images of the cerebellum. The superior view demonstrates the general relationship of lobules III to Crus I and the position of the primary fissure. Note the relatively small size of the anterior lobe. The vermis of the anterior lobe is incorporated into the hemispheres and not truly separated. The superior posterior fissure is also prominent. The posterior view demonstrates prominent superior posterior and horizontal fissures that converge near the posterior midline (b). These fissures bracket the bilateral Crus I, resulting in a 'bowtie' appearance (Crus I Bowtie Sign). The bulk of the periphery of the cerebral hemispheres is comprised of Crus I and Crus II, and to a lesser extent lobule VIIB. The remaining lobules are smaller and more medial in location. An inferior view of the cerebellum demonstrates the flocculus (lobule X) and the tonsil of lobule IX as well as lobules VIII and VIIB (c). An anterior view demonstrates the relative position of all the lobules (I–X) of the cerebellar hemispheres and the anterior vermis including the nodulus (lobule X) (d).

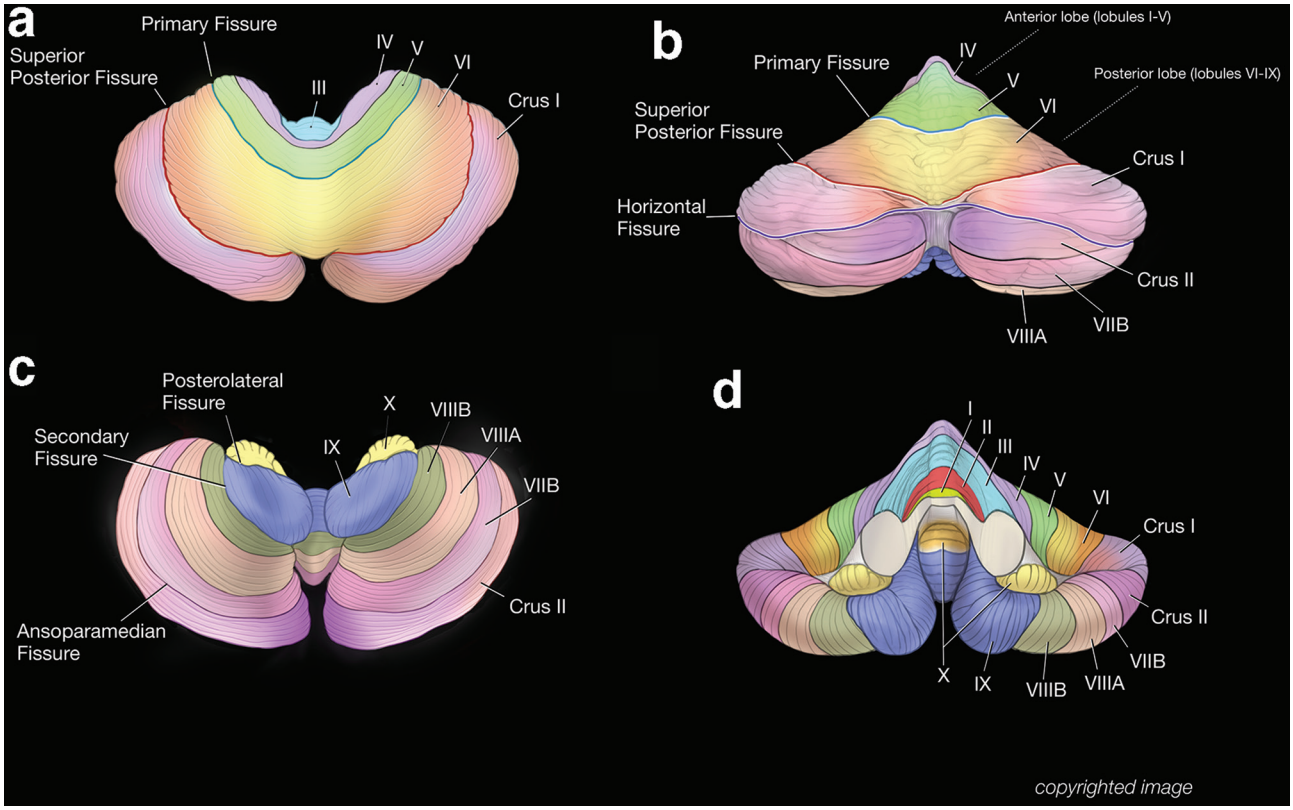


can account for numerous categories of deranged anatomy including the existence of segmental vermian abnormalities and the isolated presence of the posterior vermis in some cases of rhomboencephalosynapsis.[6] Examples of these concepts are included in Figure 6.

## DIFFUSION TENSOR IMAGING (DTI) AND TRACTOGRAPHY OF WHITE MATTER

DTI can depict areas of afferent and efferent white matter tracts of the cerebellum as well as some of the major white matter stems within the cerebellum. However, tractography techniques are needed for detailed delineation of the afferent and efferent tracts. Karavasilis et al report that both crossed and uncrossed components of the afferent tracts [fronto-ponto-cerebellar (FPC), parieto-ponto-cerebellar (PPC), occipito-ponto-cerebellar (OPC) tracts] to the cerebral hemispheres can be identified with tractography.[9] In distinction, the *uncrossed* fibers of the dentato-rubro-thalamo-cortical tract (DRTC) are most consistently depicted with current DTI and tractography techniques, although crossed fibers are more numerous (Figure 7).[9] This is important because the cerebellum and DRTC have a role in many tremor conditions and mapping the DRTC can facilitate functional neurosurgical treatment.

## OVERVIEW OF FUNCTIONAL ANATOMY

The cerebellum contributes to diverse distinct central nervous system functions including motor, language, working memory, executive function, autonomic, and affect. In general, such function demonstrates organization in a medial to lateral distribution and in a radial distribution amongst the lobules. To a first approximation, both motor and association cerebellar function demonstrate mirror-image organization about the Crus I/II expansion.[10] There is also evidence of a small tertiary map near lobule IX.[10] As exceptions, some data indicate lack of cerebellar connectivity to the primary visual and primary auditory cortex.[10] During routine clinical fMRI, cerebellar BOLD activity may be identified within the cerebellum at 3 or 7 T. Additionally, special coils and techniques to specifically assess cerebellum BOLD activity at 7 T have been described (Figure 8).[11]

Figure 3. Key sagittal MPRAGE views of the cerebellum, medial to lateral at 3 T (a–d) and 7T (e–f). Near-midline sagittal view demonstrates the vermis in native (a) and color-coded, enumerated (b) formats. The deep midline primary (light blue) and pre-pyramidal/pre-biventral (dark blue) fissures are prominent features of a normal vermis. The primary fissure separates the anterior lobe (lobules I–V) from the posterior lobe (lobules VI–IX, with lobule X constituting the flocculonodular lobe); note that the 'anterior' lobe is actually positioned superior to the posterior lobe by conventional directions used in clinical interpretation. A common dorsally directed white matter stem (red line) gives rise to lobules VI and VIIA/VIIB, whereas the remaining lobules of the vermis typically have unique white matter stems. In the mid-aspect of the cerebellar hemisphere, the primary fissure is shallow and anteriorly positioned, consistent with relatively small and medial configuration of the anterior lobe (c). The white matter stems of the Crus I (yellow) and Crus II (light blue) are clearly distinguishable. The superior posterior and horizontal fissures bracket Crus I. The far lateral aspect of the cerebellar hemisphere is composed of the Crus I/Crus II expansions along with lobule VIIB (d). The superior posterior and horizontal fissures remain clearly visible and converge anteriorly. Sagittal images in another patient at 7 T demonstrates a very similar appearance of the lobules and major fissures of the vermis (e) and the lateral cerebellar hemisphere (f) with only minor differences compared to the first patient, illustrating that these features are reasonably reproducible. Although the fine detail of the lobules and fissures are better depicted at 7 T, note that the main features are also readily identifiable at 3 T. MPRAGE, magnetization-prepared rapid acquisition with gradient echo.

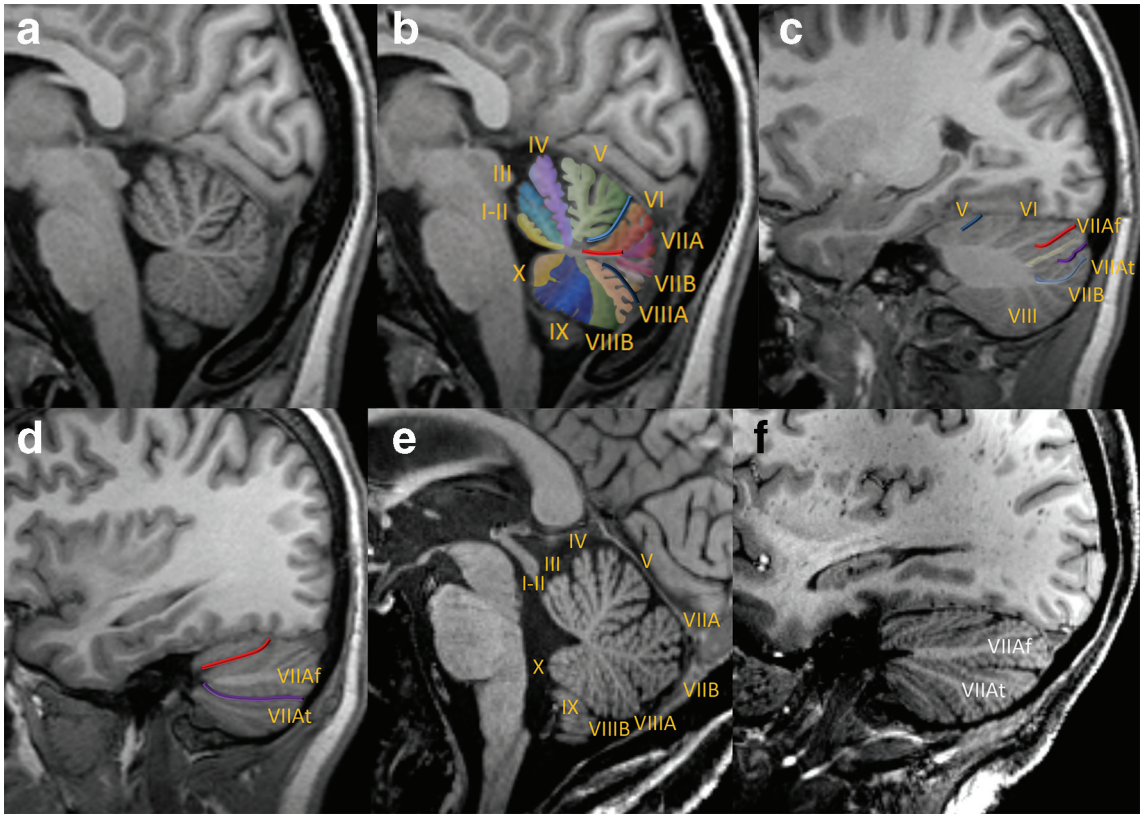


Motor function, and corresponding BOLD activity on fMRI examinations, is largely found in the anterior lobe, with additional motor function within the ventral cerebellum (particularly lobules VIII) and deep cerebellar nuclei. This motor activity demonstrates somatotopic organization both within the cerebellar hemispheres and the dorsal dentate nucleus (the ventral dentate nucleus is thought to serve largely non-motor function). Key motor function of the cerebellar cortex is medially located within the anterior lobe.

The majority of the cerebellum specializes in non-motor functions with connectivity to multimodal association areas of cerebral cortex (Figure 9). The bulk of the cerebellum is comprised of the posterior lobe and the lateral and peripheral most regions are formed by Crus I/II. The relatively expansive Crus I/II lobules demonstrate connectivity to association cerebral cortex. Overall, the size of regional connections between the cerebellum and cerebrum are relatively proportionate.[10] Specific regions of the cerebellum have been found to participate in intrinsic connectivity networks of the brain such as the default mode, salience, and executive networks.[12,13]

Language function localizes to the posterior lobe contralateral to the language dominant cerebral hemisphere, usually the right posterior lobe of the cerebellum.[14] Similarly, whereas the right cerebral association areas have a prominent role in visuospatial function, this function localizes to the left posterior cerebellar hemisphere. There is also evidence that

Figure 4. Key axial MPRAGE (a–c) and corresponding $T_2$-weighted (d–f) views of the cerebellum at 7 T, superior to inferior. In the superior cerebellum, the intraculminate fissures terminate medially in an 'X-shaped' region ('Intraculminate X' sign) of white matter (a). In distinction, the primary fissure is relatively deep and continues to extend across midline at this level just posterior the 'X.' In the mid-cerebellum, the white matter stems of Crus I (yellow) and Crus II (blue) converge medially to form a sideways 'horseshoe' configuration ('Crus Horseshoe' sign) surrounding the horizontal fissure (b). Within the vermis, a 'diamond' configuration of white matter ('Diamond' Sign) demarcates the locations of the white matter stems to lobules VIII (posterior diamond) and IX (anterior diamond). Lobule X (the nodulus) makes an impression on the fourth ventricle and is flanked by superior portions of the cerebellar tonsils (lobule IX). The relatively deep/prominent pre-pyramidal/pre-biventral fissure has a characteristic appearance with upturned anteriorly directed edges, just posterior to the 'diamond' of white mater. The biventral lobules form the ventral surface of the cerebellar hemispheres (c). The tonsils (lobule IX) extend inferomedially. Inferiorly, the horizontal fissure has a slight medial convex orientation. These same features can also be recognized on high-resolution $T_2$ weighted images, although the white matter stems demonstrate hypointense signal rather than the hyperintense signal seen on $T_1$ weighted images. Note that the hypointense white matter stem to lobule IX of the cerebellar hemisphere (white arrow) is slightly inwardly convex whereas the white matter stems to lobules VIIIB (orange arrow), VIIIA (yellow arrow), and VIIB (blue arrow) are outwardly convex (f). MPRAGE, magnetization-preparedrapid acquisition with gradient echo.

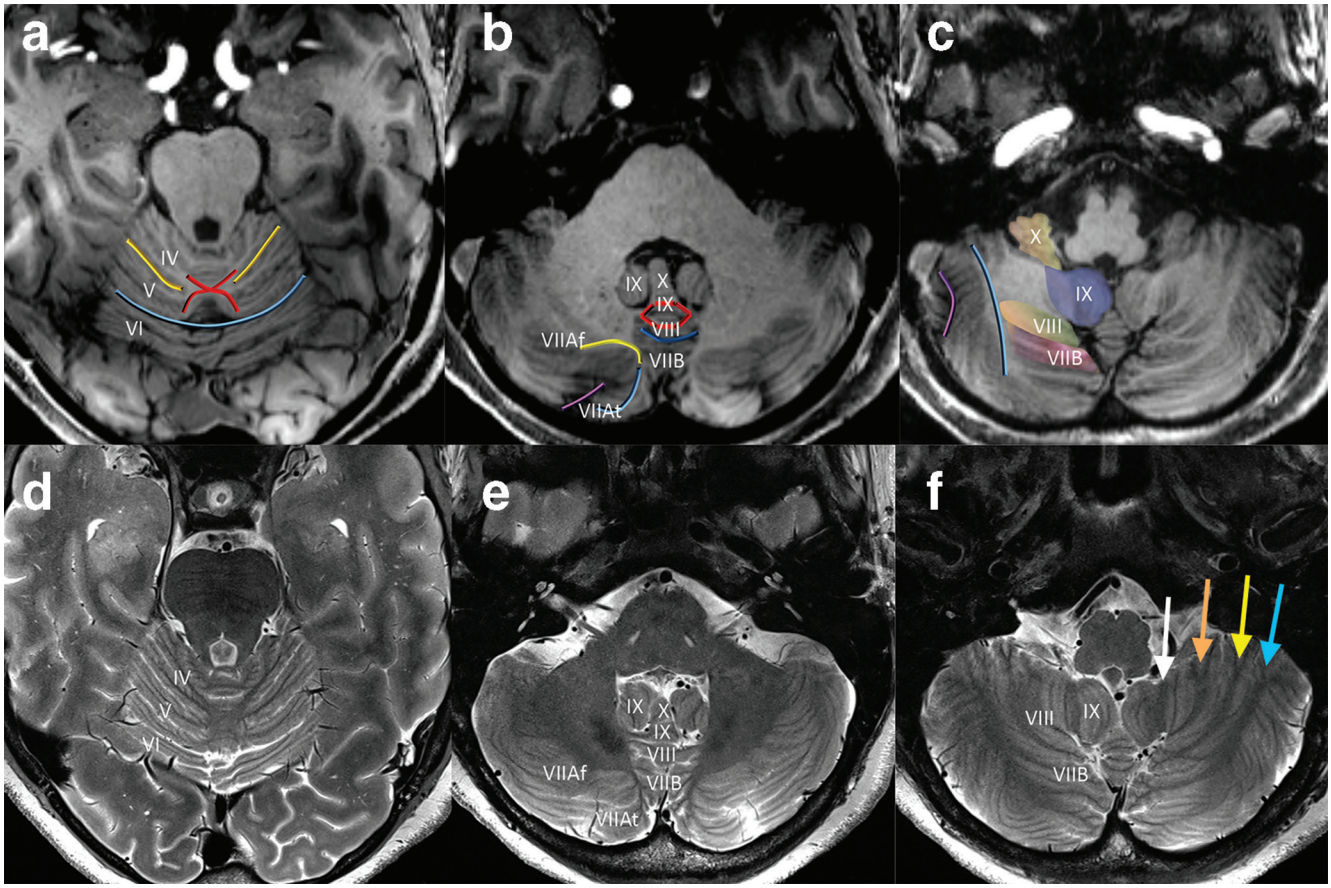


working memory function maps to the left posterior cerebellar hemisphere.

The deep cerebellar nuclei (Figure 10) also demonstrate mediolateral and rostral-caudal functional organization. In general amongst the nuclei, motor function is located medially, with truncal motor control closest to midline and lower extremity control present more off midline. Further, somatotopic organization of motor function has been described within the dorsal dentate nucleus with a rostral (foot activation) to caudal (finger activation) gradient at 7 T on group analysis, although some overlap occurred.[15]

## LESION–SYMPTOM MAPPING

Lesion involving specific regions of the cerebellar hemispheres or deep nuclei can result in specific clinical findings (Figure 11). However, such findings can be more subtle and variable than with lesions of the cerebral hemispheres and clinically detectable deficit may be absent. Studies in the human brain mapping literature have correlated the area of lesion overlap and involvement to clinical deficits in groups of patients.[16,17] In general, the resultant clinical manifestations can be predicted by knowledge of cerebellar functional topology.

Figure 5. Key coronal views of the cerebellum, posterior to anterior at 3 T (a–d) and 7 T (e). Posteriorly, the cerebellum is comprised predominantly of the Crus I and Crus II expansions (a). The white matter stems to Crus I and Crus II are well-defined and converge posteromedially along with the superior posterior and horizontal fissures. In the mid-posterior plane (b), the primary fissure is prominent and is continuous across midline (there is not a truly separate vermis superiorly in the mature cerebellum). The intraculminate fissure is also seen extending across midline superiorly. The mid-cerebellum demonstrates the majority of the lobules of the cerebellar hemispheres (c). Along the basal cerebellum, the pre-pyramidal/pre-biventral fissure typically has a slight superomedial slant while the secondary fissure has a superolateral slant. A posterior image demonstrates lateral shallow positions of the intraculminate and primary fissure (d). The floculli (lobule X) are also visualized. Afi coronal $T_2$ weighted image at 7 T in another patient at a posterior level (similar level to b) demonstrates that the major white matter stem branching pattern is reproducible, with prominent $T_2$ hypointense white matter stems to Crus I and Crus II that converge medially and a moderately prominent stem to lobule VI (e).

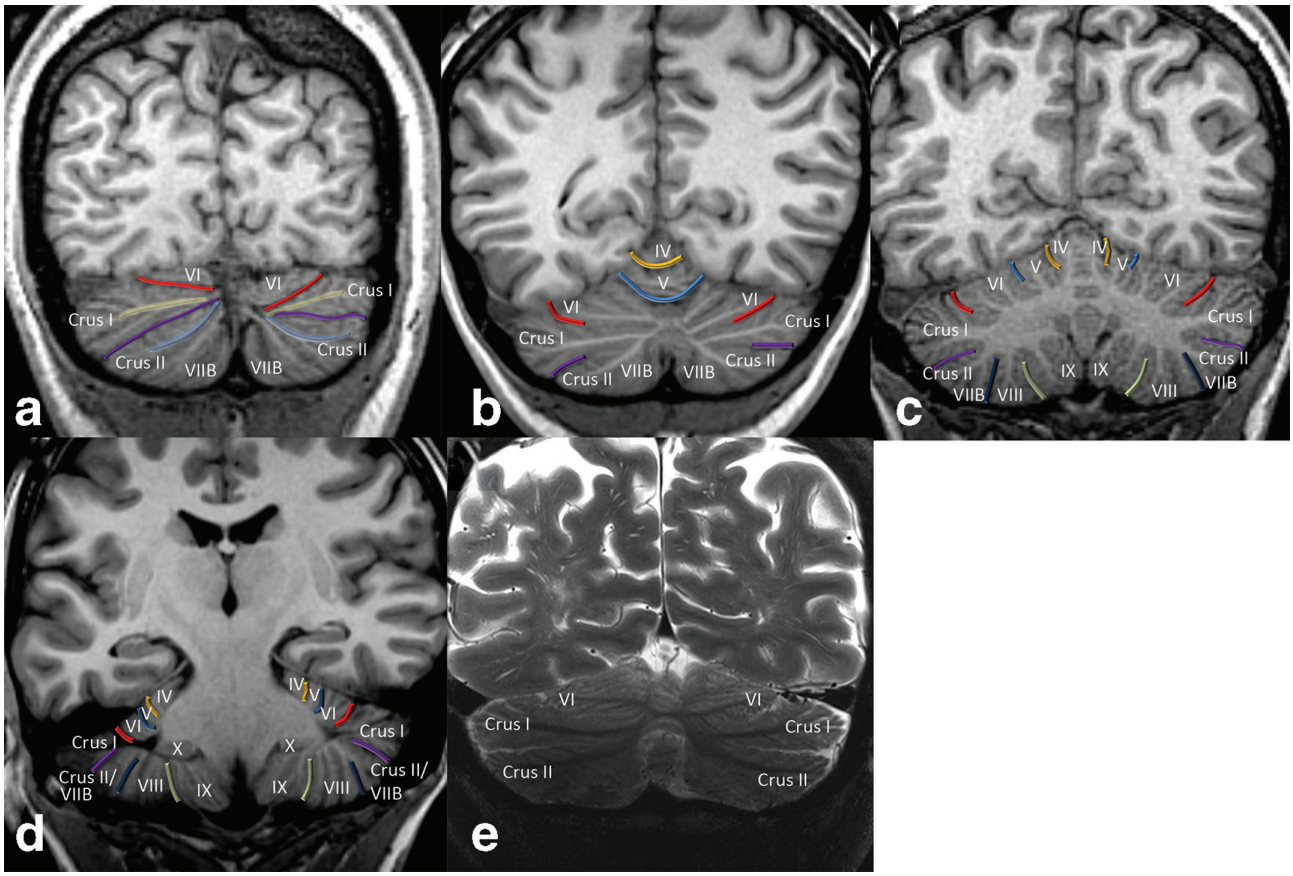


For example, lower limb ataxia can result from lesions of lobules III–IV and upper limb ataxia from lesions of lobules IV–VI. Dysarthria can result from lesions of lobules V and VI and eyeblink conditioning is altered by lesions of lobule VI and Crus I. Lesions of the deep cerebellar nuclei can also be subdivided, with lesions of the fastigial and interposed nuclei predisposing to truncal ataxia and lesions of the interposed and dentate nuclei predisposing to limb ataxia. In general, there seems to be less recovery of function in the chronic state with lesions of the deep nuclei relative to the cortex.[16,17]

Isolated acute cerebellar infarcts can provide insight into cerebellar function due to acute onset, lack of opportunity to adapt, and defined anatomic extent of pathology. Anterior lobe infarcts, which approximately correspond to the superior cerebellar artery (SCA) territory, can result in predominantly motor symptoms including dysarthria and upper and/or lower limb ataxia depending on location (Figure 11). The SCA also typically supplies the dorsal (motor) portions of the dentate nucleus whereas the posterior inferior cerebellar artery (PICA) supplies the inferior (non-motor dentate); accordingly evidence indicates the SCA infarcts with dentate involvement are associated with impaired hand gripping tests whereas PICA infarcts with dentate involvement are not.[18] However, the majority of cerebellar infarcts involve the posterior lobe (approximately anterior inferior cerebellar artery–PICA territory), which may be associated with predominantly nonspecific symptoms including nausea, headache, and confusion. Although the correlation of loss of function to area of isolated cerebellar infarct somewhat variable, in general limb ataxia and dysarthria are most common with SCA infarcts whereas gait ataxia can be seen

Figure 6. Congenital anomalies of the cerebellum in three patients. First, a 53-year-old female with extension of cerebellar hemisphere folia continuously across midline with absent vermis indicating classic rhombencephalosynapsis, an abnormality of dorsoventral patterning (a–c).[8] The superior cerebellar peduncles are fused posteriorly (white arrows, a) and the deep cerebellar nuclei appear fused (white arrows, b). Inferiorly, the vermis is completely absent (c), although in cases of incomplete rhomboencephalosynapsis, the inferior vermis is present. This condition is associated with highly variable cognitive and motor deficits. This patient was a high-functioning professional with mild ataxia on exam. Another case demonstrates vermian hypoplasia in a 5-year-old (d). The vermis is small with superiorly positioned inferior border (white arrows); a dorsally directed white matter stem consistent with a stem to lobules VI, VIIa, and VIIb flanked by the prominent primary and pre-pyramidal/pre-biventral fissures are present while the lobules while the number of white matter stems to the remaining areas of the anterior and posterior lobe are more difficult to identify. On overall semblance of typical lobulation remains present, compatible with hypoplasia whereas lack of normal lobulation would indicate dysgenesis. A third case demonstrates hypoplasia of both the cerebellum and pons in a 1-year-old (e–f). The vermis is hypoplastic and the pons is markedly hypoplastic (e). Laterally on the right, the cerebellar hemisphere is also small, although the fissures are not widened (f); decreased size due to widening of otherwise normal fissures would indicate atrophy rather than hypoplasia. Note that the white matter stems to Crus I and crus II remain identifiable. Hypoplasia of the pons frequently accompanies that of the cerebellum due to shared developmental origins and/or white matter circuitry.[8]

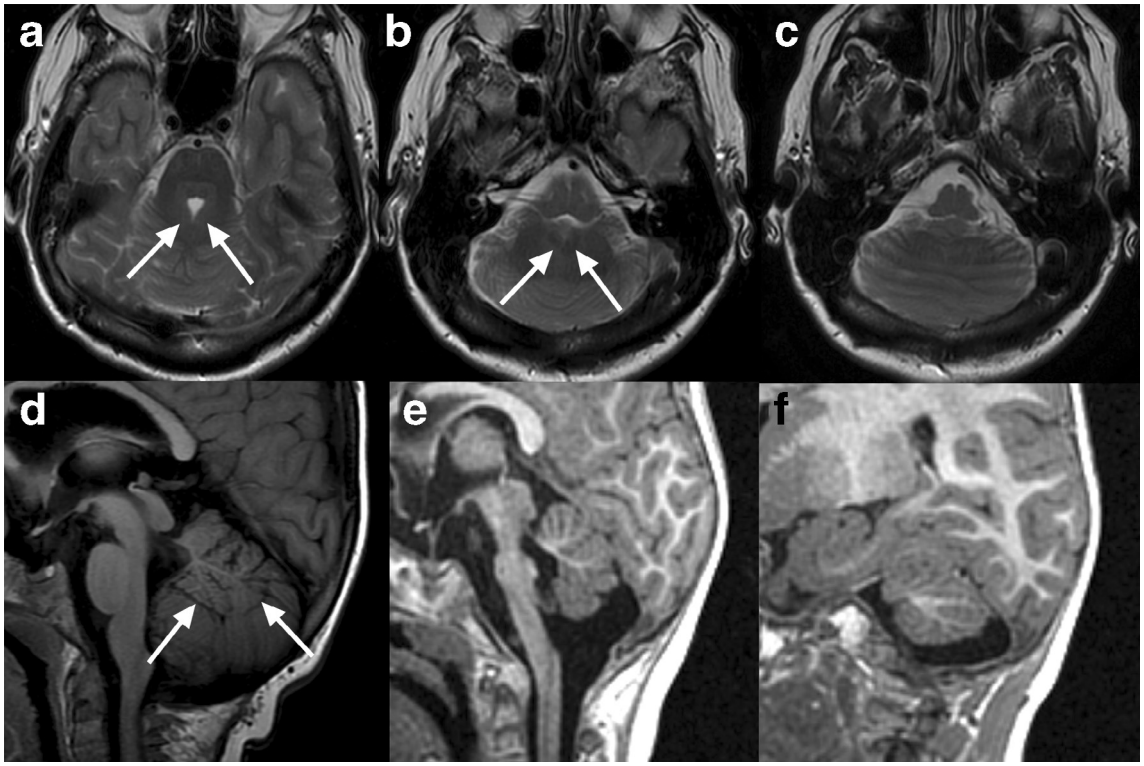


with SCA or PICA infarcts, in particular with involvement of the vermis.[16,19,20]

Lesion–symptom mapping can also be predicated upon long-standing pathology and the effects of surgical resection. For example, there is evidence that resection of tumors from the posterior lobes can result in impaired cognition, affect, and pain processing and that resection of medulloblastomas of the left posterior cerebellar lobe is associated with decreased working memory.[21,22] Schmahmann et al described the cerebellar cognitive affective disorder, which encompasses a variety of executive function and behavioral symptoms due to lesions of the posterior lobes.[17] This can include planning, reasoning, working memory, language, personality, affect, and altered behavior.

## PATHOLOGIC DERANGEMENT

With symptom–lesion mapping, study of normal function and structure can facilitate an understanding of clinical manifestations of pathology. Both intrinsic derangement within the cerebellum itself and altered functional connectivity due to pathology of the cerebral hemisphere are possible. Altered structure and function can be on either an acquired or a congenital basis (Figures 12–13).

## KEY TAKE HOME POINTS

(1) Advances in the human brain mapping literature in recent decades have substantially improved the understanding of cross-sectional and functional anatomy of the cerebellum.

Figure 7. Tractography at the level of the anterior commissure-posterior commissure line demonstrates the DRTC (purple) at the level of the inferior VIM, the somatomotor tract (yellow), and somatosensory/medial lemniscus fibers (red) near the ventral caudal nucleus in the thalamus in a patient with right essential tremor (a). Note the close proximity of these three tracts. The VIM was successfully targeted by MRI-guided focused ultrasound for treatment of right essential tremor, avoiding the other two tracts. Although most white matter fibers to the DRTC arise from the contralateral cerebellar nuclei, current standard clinical DTI/tractography techniques most often identify fibers arising from the *ipsilateral* dentate nucleus via the ipsilateral superior cerebellar peduncle. Directionally encoded fractional anisotropy images demonstrate a region of dark purple color (lavender arrow) within the thalamus that corresponds to the DRTC and the somatosensory fibers (b), although these two tracts cannot be confidently differentiated; this is just medial to the posterior limb of the internal capsule, which is blue (blue arrow), while the thalamus anterior and medial to this region is green. At the level of the upper midbrain (c), most fibers of the DRTC extend across midline within the decussation of the superior cerebellar peduncles (red arrow), although some fibers remain ipsilateral. At the level of the superior cerebellar peduncles (d), efferent cerebellar white matter tracts, including the DRTC, are seen in light blue color (white arrow). Just inferior to this (e), the DRTC fibers merge with a green area in this patient (color varies amongst patients) (white arrow) along the medial aspect of the dentate nucleus. At this level, red transverse pontine fibers containing the FPC, PPC, and OPC tracts are also visualized (yellow arrow) as well as the middle cerebellar peduncle (green arrow). In the mid to inferior cerebellum, the white matter stems to Crus I and Crus II are often seen as green tracts (orange arrow denotes stem to crus II) (f). DRTC,dentato-rubro-thalamo-cortical tract; DTI, diffusiontensor imaging; FPC, fronto-ponto-cerebellar;OPC, occipito-ponto-cerebellar; PPC, parieto-ponto-cerebellar; VIM, ventral intermediate nucleus.

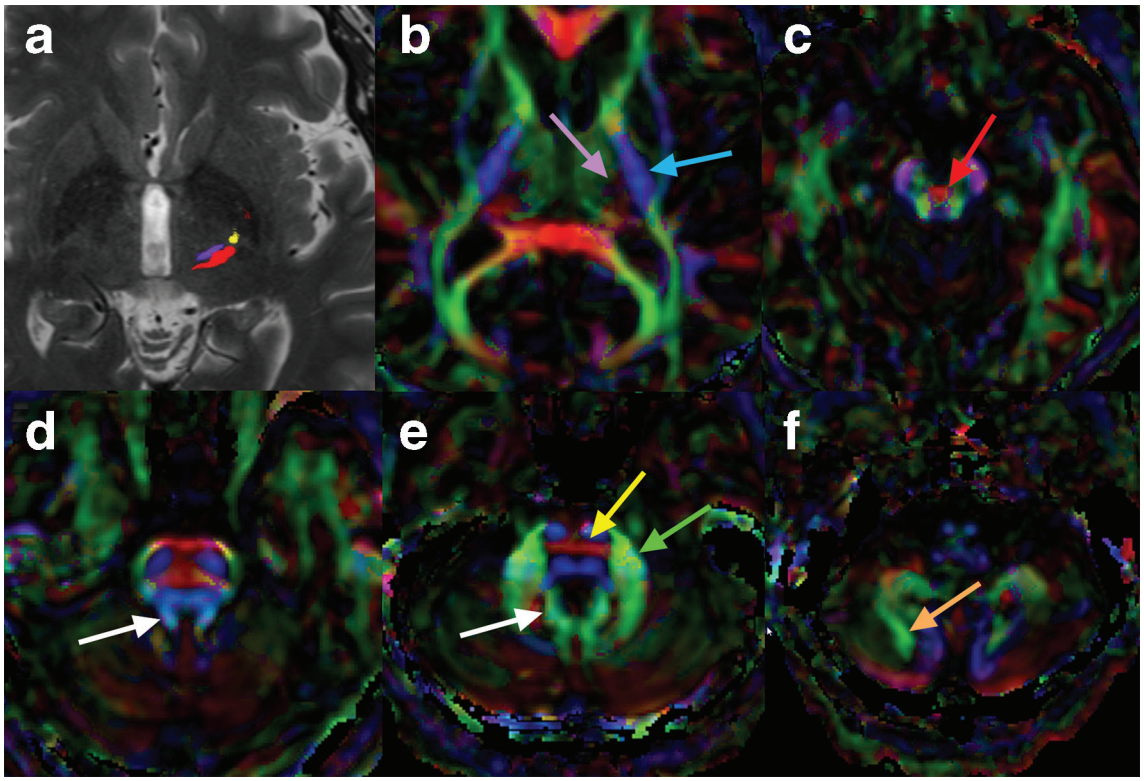


(2) Numerical lobule designation per the Schmahmann classification is arranged radially in the sagittal plane. Most lobules of the vermis are identified by an independent white matter stem, whereas lobules VI, VIIA, and VIIB have a common dorsally directed stem and are the last to differentiate.

(3) The main anatomic features of the cerebellum on MRI can be recognized by relationship to several typical white matter stem and fissure configurations, orientations, and/or prominence. Key signs include the **'intraculminate X sign'** just anterior to the deep primary fissure and the **'crus I bowtie sign'** amongst many others described herein.

(4) Lesion–symptom mapping reports indicate that lesions of the anterior lobe can result predominantly in motor deficits and specific forms of ataxia corresponding to homunculus involvement whereas lesions of the larger posterior lobe can result in nonmotor symptoms such as cerebellarcognitive affective disorder and impaired working memory. Nonetheless, lesions of the cerebellum often result in a variety of non-specific symptoms. Lesions of the deep nuclei are important to recognize since there is generally less recovery of function over time compared to other regions of the cerebellum.

Figure 8. BOLD activity in the cerebellum derived from clinical fMRI examinations at 3 and 7 T. Somatotopic organization of motor function of the anterior cerebellum lobe can be resolved at 3 T (a). Tongue activation (green) is seen posteriorly near the primary fissure (blue arrow), toe tapping (magenta) activation is seen anteriorly, and activation related to finger tasks is seen in the mid-portion of the anterior lobe. This follows the cerebellar homunculus. Motor activity in the anterior cerebellar hemisphere can be exquisitely demonstrated with bilateral hand clenching at 7 T (b). Silent word generation produces activity consistent with bilateral lip motor function in the bilateral anterior lobes at 3 T (c). Expressive language tasks also often produce tongue/lip motor activation thought to be related to 'silent word' generation during the task (yellow). Left occipital lobe visual cortex activity also incidentally depicted. Additional language tasks (rhyming task = blue; reading comprehension task = green; semantic decision task = magenta; silent word generation task = yellow) with activity co-localizing to right posterior cerebellar lobe spanning Crus I and II (same patient as c) (d). This patient has strong *left* cerebral hemisphere language dominance on fMRI (not shown). BOLD, blood oxygen level dependent.

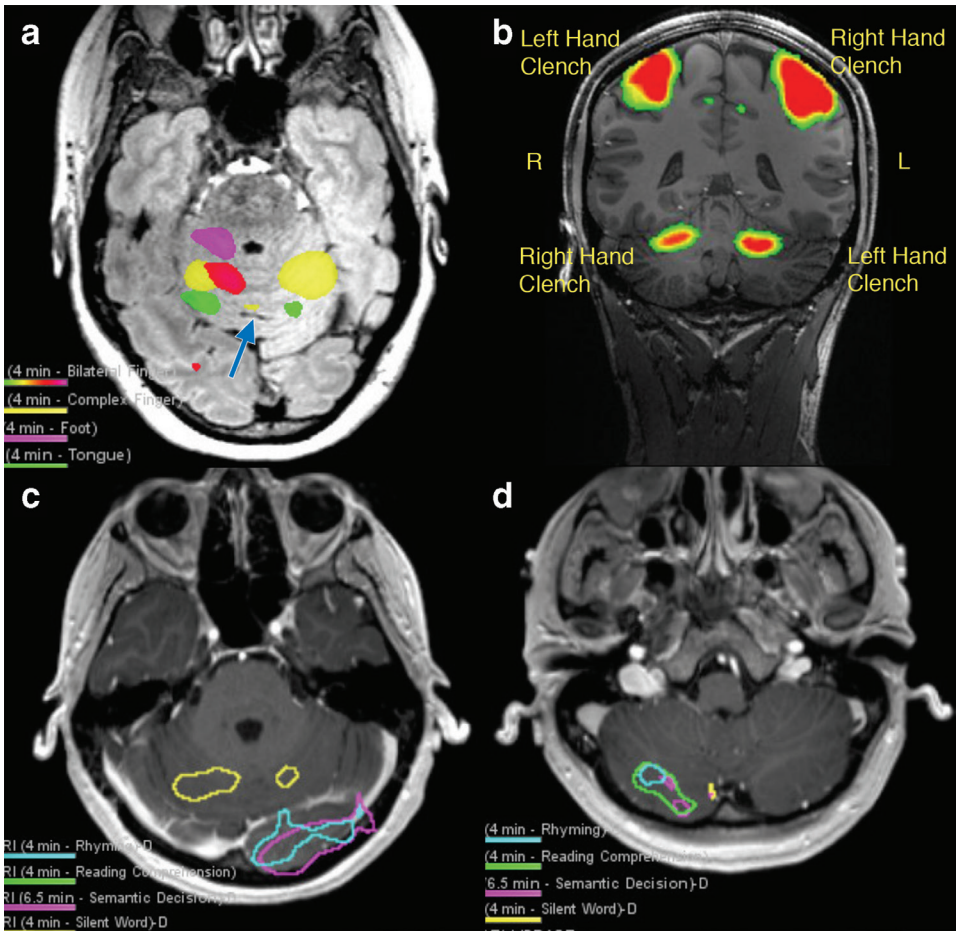


Figure 9. Color-coded illustration of approximate pattern of *general* regions of connectivity between the cerebral and cerebellar hemispheres, including a 3D-rendered image based on MPRAGE (a), a select coronal (b) and a select axial (c) image from the same patient. Regions of matching color in the cerebrum and cerebellum have been shown to have functional connectivity. Note connectivity of the somatomotor areas to the anterior lobe and lobules VIII and larger areas of connectivity of multimodal association areas to the lateral expansive portions of the cerebellar hemispheres. According to and modified from Buckner et al.[10] MPRAGE, magnetization-preparedrapid acquisition with gradient echo.

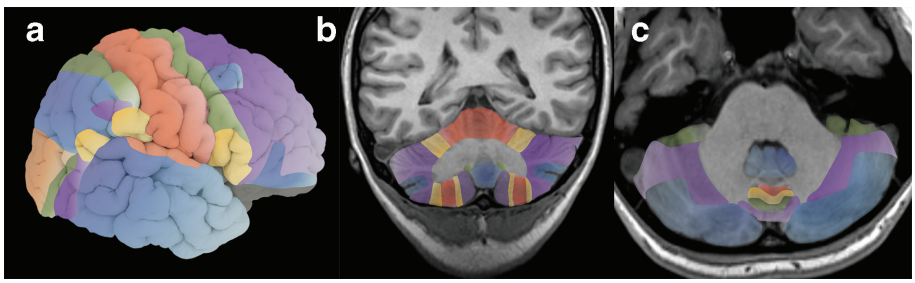

Figure 10. Cerebellar nuclei are hypointense on SWI at 7 T. The dentate nucleus is well-delineated while the general locations of the other nuclei can be inferred on visual inspection. The paired fastigial nuclei are near midline, located along the roof of the fourth ventricle (white arrow) (a). The interposed nuclei (globose and emboliform) are not always distinguishable, but located near the dorsomedial border of the dentate nucleus and should be approximated by the labelled structure (white arrow) (b). Ventrally, the normal peripherally crenulated appearance of the dentate nuclei is well seen (white arrow) (c). An incidental cavernous malformation in the pons is also present. SWI,susceptibility-weighted imaging.

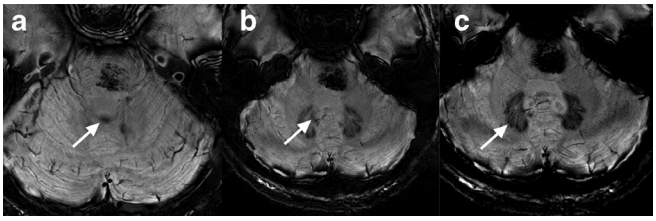


Figure 11. Key approximate areas identified in cerebellar lesion–symptom mapping literature on axial 7 T MPRAGE images (a–d). Motor manifestations predominantly involve the anterior lobe and can be roughly predicted by knowledge of somatotopic organization. The upper limb ataxia region primarily involves the anterior lobe, but extends slightly over the primary fissure to the posterior lobe. Cerebellar dysarthria and abnormal eyeblink conditioning reportedly extend across the primary fissure. Eyeblink conditioning has also been mapped to Crus I. Truncal ataxia maps to the medial cerebellum throughout the majority of the vermis. Non-motor consequences such as CCAS map to areas of the posterior lobe. The intraculminate (black arrow), primary (white arrow), and horizontal (peach arrow) fissures as well as the white matter stems to Crus I (yellow arrow) and Crus II (blue arrow) are labelled. Images are modified from Timmann et al.[16] CCAS,cerebellar cognitive affective disorder; MPRAGE, magnetization-prepared rapidacquisition with gradient echo.

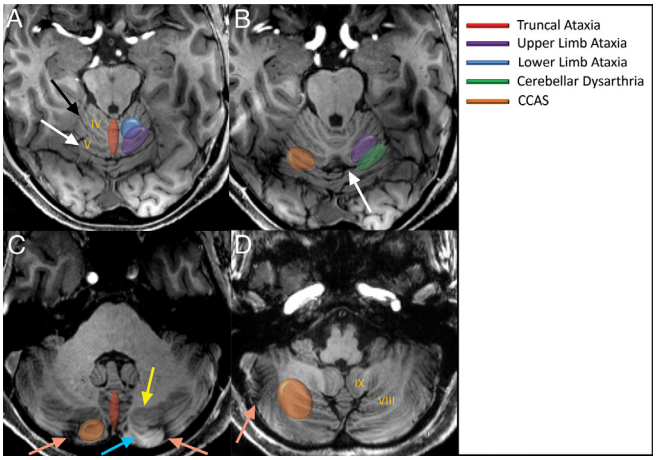


Figure 12. Example of altered cerebral–cerebellar functional connectivity due to a congenital lesion in the cerebral hemisphere. This patient has schizencephaly in the right primary somatomotor region (arrow) (a, b). BOLD activity on motor tasks indicates that both right and left somatomotor function (red = bilateral finger task with alternating sides, green = tongue task, blue = lip task) is served by the anatomically normal left cerebral hemisphere (a, b). There was no evidence of neurovascular uncoupling in the right cerebral hemisphere (not shown). Corresponding BOLD activity is present in the right cerebellar hemisphere, with bilateral finger tapping depicted (red) (c). There was no appreciable BOLD activity in the expected somatomotor areas of the right cerebral or left cerebellar hemispheres. BOLD,blood oxygen level dependent.

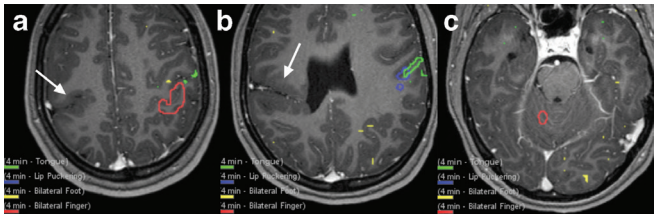


(5) The cerebellum plays a role in tremor syndromes and DRTC tractography, including that of uncrossing fibers, can facilitate functional neurosurgical treatment.

Figure 13. Decreased size of a cerebellar nucleus due to involvement with pathology of a brainstem–cerebellum circuit (triangle of Mollaret) with associated decreased accumulation of gadolinium. Asymmetrically $T_1$ hyperintense dentate nucleus in a 32-year-old female with history of right hypertrophic olivary degeneration and administration of multiple i.v. gadolinium doses. The right dentate nucleus demonstrates $T_1$ hyperintensity (white arrow) which can be seen after gadolinium administration, and normal size. The left dentate nucleus is atrophic and difficult to visualize, consistent with involvement with hypertrophic olivary degeneration, and demonstrates less intense $T_1$ signal.

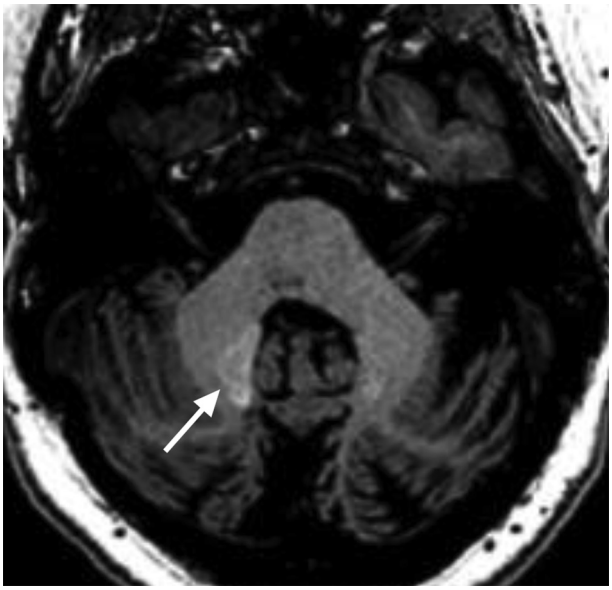

(6) Normal and pathologic anatomy and function of the cerebellum is intertwined with the brainstem and cerebrum via circuits. Cerebellar pathology can arise from insults primary to these other locations such as malformations of cerebral cortical development.

## ACKNOWLEDGMENT

The authors acknowledge the assistance of Sonia Watson, PhD, in editing the manuscript.

## CONFLICTS OF INTEREST

TJK: Consult for SpineThera and stock option ownership, not relevant to current work; all other authors have no conflicts of interest to declare.

## REFERENCES

1. Apps R, Hawkes R, Aoki S, Bengtsson F, Brown AM, Chen G, et al. Cerebellar Modules and Their Role as Operational Cerebellar Processing Units: A Consensus paper [corrected. *Cerebellum* 2018; **17**: 654–82. doi: https://doi.org/10.1007/s12311-018-0952-3
2. Marques JP, van der Zwaag W, Granziera C, Krueger G, Gruetter R. Cerebellar cortical layers: in vivo visualization with structural high-field-strength MR imaging. *Radiology* 2010; **254**: 942–8. doi: https://doi.org/10.1148/radiol.09091136
3. Diedrichsen J, Maderwald S, Küper M, Thürling M, Rabe K, Gizewski ER, et al. Imaging the deep cerebellar nuclei: a probabilistic atlas and normalization procedure. *Neuroimage* 2011; **54**: 1786–94. doi: https://doi.org/10.1016/j.neuroimage.2010.10.035
4. Maderwald S, Thürling M, Küper M, Theysohn N, Müller O, Beck A, et al. Direct visualization of cerebellar nuclei in patients with focal cerebellar lesions and its application for lesion-symptom mapping. *Neuroimage* 2012; **63**: 1421–31. doi: https://doi.org/10.1016/j.neuroimage.2012.07.063
5. Schmahmann JD, Doyon J, Petrides M, Evans A, Toga A. *MRI Atlas of the Human Cerebellum*: Academic Press; 2000.
6. Robinson AJ. Inferior vermian hypoplasia--preconception, misconception. *Ultrasound Obstet Gynecol* 2014; **43**: 123–36. doi: https://doi.org/10.1002/uog.13296
7. Yang Z, Ye C, Bogovic JA, Carass A, Jedynak BM, Ying SH, et al. Automated cerebellar lobule segmentation with application to cerebellar structural analysis in cerebellar disease. *Neuroimage* 2016; **127**: 435–44. doi: https://doi.org/10.1016/j.neuroimage.2015.09.032
8. Barkovich AJ, Millen KJ, Dobyns WB. A developmental and genetic classification for midbrain-hindbrain malformations. *Brain* 2009; **132**(Pt 12): 3199–230. doi: https://doi.org/10.1093/brain/awp247
9. Karavasilis E, Christidi F, Velonakis G, Giavri Z, Kelekis NL, Efstathopoulos EP, et al. Ipsilateral and contralateral cerebro-cerebellar white matter connections: a diffusion tensor imaging study in healthy adults. *J Neuroradiol* 2019; **46**: 52–60. doi: https://doi.org/10.1016/j.neurad.2018.07.004
10. Buckner RL, Krienen FM, Castellanos A, Diaz JC, Yeo BTT. The organization of the human cerebellum estimated by intrinsic functional connectivity. *J Neurophysiol* 2011; **106**: 2322–45. doi: https://doi.org/10.1152/jn.00339.2011
11. Batson MA, Petridou N, Klomp DWJ, Frens MA, Neggers SFW. Single session imaging of cerebellum at 7 Tesla: obtaining structure and function of multiple motor subsystems in individual subjects. *PLoS One* 2015; **10**: e0134933. doi: https://doi.org/10.1371/journal.pone.0134933
12. Bernard JA, Seidler RD, Hassevoort KM, Benson BL, Welsh RC, Wiggins JL, et al. Resting state cortico-cerebellar functional connectivity networks: a comparison of anatomical and self-organizing map approaches. *Front Neuroanat* 2012; **6**: 31. doi: https://doi.org/10.3389/fnana.2012.00031
13. Habas C, Kamdar N, Nguyen D, Prater K, Beckmann CF, Menon V, et al. Distinct cerebellar contributions to intrinsic connectivity networks. *J Neurosci* 2009; **29**: 8586–94. doi: https://doi.org/10.1523/JNEUROSCI.1868-09.2009
14. Jansen A, Flöel A, Van Randenborgh J, Konrad C, Rotte M, Förster A-F, et al. Crossed cerebro-cerebellar language dominance. *Hum Brain Mapp* 2005; **24**: 165–72. doi: https://doi.org/10.1002/hbm.20077
15. Küper M, Thürling M, Stefanescu R, Maderwald S, Roths J, Elles HG, et al. Evidence for a motor somatotopy in the cerebellar dentate nucleus--an FMRI study in humans. *Hum Brain Mapp* 2012; **33**: 2741–9. doi: https://doi.org/10.1002/hbm.21400
16. Timmann D, Brandauer B, Hermsdörfer J, Ilg W, Konczak J, Gerwig M, et al. Lesion-symptom mapping of the human cerebellum. *Cerebellum* 2008; **7**: 602–6. doi: https://doi.org/10.1007/s12311-008-0066-4
17. Stoodley CJ, MacMore JP, Makris N, Sherman JC, Schmahmann JD. Location of lesion determines motor vs. cognitive consequences in patients with cerebellar stroke. *Neuroimage Clin* 2016; **12**: 765–75. doi: https://doi.org/10.1016/j.nicl.2016.10.013
18. Kim S, Lee H, Lee Y, Lee J, Yang J, Lee M, et al. Blood supply by the superior cerebellar artery and posterior inferior cerebellar artery to the motor and nonmotor domains of the human dentate nucleus. *World Neurosurg* 2019; **122**: e606–11. doi: https://doi.org/10.1016/j.wneu.2018.10.111
19. De Cocker LJL, Geerlings MI, Hartkamp NS, Grool AM, Mali WP, Van der Graaf Y, et al. Cerebellar infarct patterns: the SMART-Medea study. *Neuroimage Clin* 2015; **8**: 314–21. doi: https://doi.org/10.1016/j.nicl.2015.02.001
20. Deluca C, Moretto G, Di Matteo A, Cappellari M, Basile A, Bonifati DM, et al. Ataxia in posterior circulation stroke: clinical-MRI correlations. *J Neurol Sci* 2011; **300**(1-2): 39–46. doi: https://doi.org/10.1016/j.jns.2010.10.005
21. Hoang DH, Pagnier A, Cousin E, Guichardet K, Schiff I, Icher C, et al. Anatomo-functional study of the cerebellum in working memory in children treated for medulloblastoma. *J Neuroradiol* 2019; **46**: 207–13. doi: https://doi.org/10.1016/j.neurad.2019.01.093
22. Silva KE, Rosner J, Ullrich NJ, Chordas C, Manley PE, Moulton EA. Pain affect disrupted in children with posterior cerebellar tumor resection. *Ann Clin Transl Neurol* 2019; **6**: 344–54. doi: https://doi.org/10.1002/acn3.709